Structural Characterization and Antibacterial, Antifungal, Antioxidant Activity of ONO Salicyl Based Schiff Base and its VO(II), Fe(III), Co(II), Ni(II), Cu(II), Zn(II), Pd(II) and Hg(II) Complexes

Dildora Pardaeva[a], Aydin Tavman[b*], Erol Erçag[c], Mayram Hacioglu[d], Demet Gürbüz[e], Adem Çinarli[e], A. Seher Birteksöz Tan[d]

[a] *Istanbul University-Cerrahpaşa, Institute of Graduate Education, Department of Chemistry, 34320, Avcilar, Istanbul, Türkiye.*

[b] *Istanbul University-Cerrahpaşa, Faculty of Engineering, Department of Chemistry, Inorganic Chemistry Division, 34320, Avcilar, Istanbul, Türkiye*

[c] *Istanbul University-Cerrahpaşa, Faculty of Engineering, Department of Chemistry, Analytic Chemistry Division, 34320, Avcilar, Istanbul, Türkiye*

[d] *Istanbul University, Faculty of Pharmacy, Department of Pharmaceutical Microbiology, 34452, Beyazit, Istanbul, Türkiye*

[e] *Istanbul University-Cerrahpaşa, Faculty of Engineering, Department of Chemistry, Organic Chemistry Division, 34320, Avcilar, Istanbul, Türkiye*

atavman@iuc.edu.tr

Keywords: *Schiff base, salicyl, metal complex, antimicrobial, antioxidant.*

An ONO tridentate Schiff base derived from 3,5-dichlorosalicylaldehyde and 2-amino-4-methylphenol (**H_2L**) and its complexes with VO(II), Fe(III), Co(II), Ni(II), Cu(II), Zn(II), Pd(II) and Hg(II) were synthesized and characterized. The structures of the complexes were confirmed by means of elemental analysis, molar conductivity, magnetic moment, UV-visible, fluorescence, FT-IR and NMR spectroscopy. The M:L ratio is 1:2 in Fe(III) and Co(II) complexes whereas 1:1 in the other complexes. It was observed that the Pd(II) complex is 1:1 ionic while the others are non-ionic according to molar conductivity measurements. **H_2L** showed weak fluorescence at different wavelengths in neutral, acidic and basic areas and in the form of some metal complexes. The VO(II) and Cu(II) complexes increased the fluorescence effect compared to the ligand, while the Fe(III) complex completely quenched it. Antibacterial and antifungal activity of the compounds was evaluated against six bacteria and three fungi. In general, all the compounds showed moderate antimicrobial activity. It was observed that some of the complexes exhibited higher activity towards *S. epidermidis* and *S. aureus* compared to the ligand. Antioxidant activity of the compounds was investigated in terms of 1,1-diphenyl-2-picrylhydrazyl radical (DPPH•) scavenging and Cupric

Reducing Antioxidant Capacity (CUPRAC) methods. It was found that Zn(II) and Pd(II) complexes showed higher antioxidant activity than the ligand and the other complexes.

Introduction

Imine compounds, also known as Schiff bases, are one of the research topics of high interest due to their wide range of application possibilities. For example, it was reported that some Schiff bases derived from 1- alkylisatin and isonicotinic acid hydrazide showed antitubercular activity [1]. 3-(2-(4-nitrophenyl)hydrazono) indolin-2-one [2] and Schiff bases of hydroxysemicarbazide inhibited considerable antitumor activity [3]. There are studies showing that many Schiff base derivatives have antibacterial, antiviral, antifungal, anti-inflammatory, analgesic, anticonvulsant, antioxidant, antihelmintic, antimalarial and anti-HIV effects [4–8].

Additionally, Schiff bases are a group of compounds that have attracted high interest from researchers as ligands in coordination chemistry due to their high donor properties and being chelating agents [9–12]. There are studies that complexes of some transition metal ions and Schiff bases have various applications in fields such as homogeneous and heterogeneous catalysis [13–16], analytical reagents [17,18], dyeing of textile fabrics [19,20], etc. Numerous Schiff bases and some of their metal complexes, especially those with first-row transition metal ions, have been and are being studied because of their important and interesting properties such as their complexing capacity, photochromic properties and the removal of some toxic metal ions due to their reversible oxygen binding ability [21–24].

Schiff bases derived from o-aminophenol and salicylaldehyde derivatives are a class of compounds of high interest because of their forming chelate structures and variety of uses and interesting properties [25–27]. The simplest example of this class compound is "2-{[(2-hydroxyphenyl)imino]methyl}phenol". They exhibit high complexation effect and form strong chelate complexes due to their tridentate properties [28–30]. As is known, some metal ions such as Co(II), Fe(II/III), Cu(II) and Zn(II) have important roles in human body. There are also studies on the use of various Schiff bases with fluorescent properties in metal detection [31–33]. In this study, VO(II), Fe(III), Co(II), Ni(II), Cu(II), Zn(II), Pd(II) and Hg(II) complexes of a salicyl based imine compound (Schiff base) derived from 3,5-dichlorosalicylaldehyde and 4-methyl-2-aminophenol (**H_2L**) were prepared and characterized. The fluorescence behavior of **H_2L**, which has weak fluorescence properties, in acidic, basic and neutral environments and against metal ions was examined. In addition, antibacterial, antifungal, antiviral and antioxidant activities of the compounds were tested. The structural characteristics and

antimicrobial activity of **H_2L** and its complexes were evaluated.

Experimental part

Chemistry and Apparatus

All chemicals and solvents were of reagent grade and they were used without further purification.

The devices and techniques used are following: Elemental analysis: LECO combustion analyzer CHNS-932 (METU Central Laboratory). Melting points: Buchi M-560 melting-point apparatus. Molar conductivity: WTW Cond315i conductivity meter (in DMF at 25 °C). Magnetic measurements: MK1 Sherwood Scientific apparatus (at room temperature by Gouy's method). NMR spectroscopy: Varian Unity Inova 500 NMR spectrometer. FT-IR spectroscopy: Bruker Optics Vertex 70 spectrometer with Attenuated Total Reflection (ATR) techniques, between 400 and 4000 cm^{-1}. UV-Visible spectra: Shimadzu UV-1800 Spectrophotometer. Fluorescence spectra: Shimadzu RF-5301 PC Spectrofluorophotometer (in EtOH, $c = 1 \times 10^{-4}$ mol/L).

*Synthesis of 2-{(E)-[(5-methyl-2-hydroxyphenyl)imino]methyl}-4,6-dichlorophenol (**H_2L, Figure 1**)*

3,5-Dichlorosalicyladehyde (1.92 g, 10 mmol) and 2-amino-4-methylphenol (1.23 g, 10 mmol) were separately dissolved in absolute ethanol (10 mL), then they were mixed. The color of the mixture immediately turned reddish orange and clouding occurred. The molar value of the ligand is 0.5 M (10 mmol ligand / 20 mL solvent). The mixture was refluxed for 3 h, then was cooled at room temperature and filtered. After a few days, the crystals formed in the filtrate were filtered and dried at room temperature.

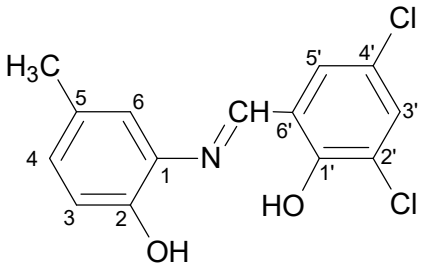

Figure 1. Chemical structure **H_2L**

Dark orange solid. Yield: 2.13 g (72%). M.p.: 261 °C. Found: C, 56.65; H, 3.81; N, 4.82%. Anal. calcd. for $C_{14}H_{11}Cl_2NO_2$ (296.15); C, 56.78; H, 3.74; N, 4.73%. MS (ESI, m/z): 292.2 ($[M]^+$, 100%), 298.2 ($[M+2]^+$, 67.0%). FT-IR Spectra (ATR, cm^{-1}): 3192 m,br ν(OH), 3065 m $\nu(CH)_{ar.}$, 2922 m $\nu(CH)_{al.}$, 1636 m ν(C=N), 1615 m ν(C=C), 1498 s, 1343 m, 1277 m, 1200 m ν(C–O), 1141 m, 1011 m, 851 m, 811 s $\delta(CH)_{ar.}$, 750 m ν(C–Cl), 667 m, 582 m, 547 m, 462 m, 435 m. ^{1}H-NMR (ppm, 500 MHz, in DMSO-d_6): 9.98 s (1H, OH2), 9.08 s (1H, N=CH), 7.65 d (H, J=2.9, H4'), 7.60 d (1H, J=2.9, H6'), 7.34 d (1H, J=1.0, H3), 7.01 dd (1H, J=8.5, 8.3, 1.5, 1.4, H5), 6.90 d (1H, J=8.3, H6), 2.27 s (3H, -CH_3). ^{13}C-NMR (ppm, 125 MHz, in

DMSO-d_6): 160.4 (N=CH), 158.9 (C–OH(2)), 149.1 (C–OH(1')), 132.8 (C–N=CH), 130.9 (C–CH_3), 130.7 (C4'), 130.1 (C5), 129.0 (C6'), 123.6 (C5'), 120.1 (C3'), 119.8 (C3), 119.6 (C1'), 117.0 (C6), 20.7 (CH_3). UV-vis spectra (in EtOH, λ_{max}/nm): 204 m, 215 m, 244 sh, 306 w,br, 361 m,br, 469 m,br, 497 sh. Fluorescence spectra (λ_{max}/nm): 547 w,br (neutral), 472 m,br (acidic), 505 m,br (basic).

Synthesis of the Complex Compounds

Appropriate metal salt solutions (1 mmol of $VOSO_4$, $FeCl_3$, $CuCl_2$ and $HgCl_2$ in MeOH; Co(II), Ni(II) and Zn(II) chlorides in 10 mL ethyl acetate; K_2PdCl_4 in 10 mL H_2O+MeOH mixture, 3+8, v/v) were added gradually to a solution of **H_2L** (1 mmol, 296 mg) in corresponding solvent (10 mL) in the molar ratio 1:1, and heated to reflux for 3 hours (Metal salt and the ligand concentrations: ~0.05 M). Cu(II) and Pd(II) salts immediately precipitated with the ligand. The other complex solutions were kept at room temperature, precipitates formed within a few days. Since the formation of Co(II), Ni(II) and Zn(II) complexes did not occur at the pH value of the mixture, which was around 4.5, the pH of the medium was brought to the range of 5.5-6.0 by using 5% NaOH methanolic solution to ensure the formation of complexes. The precipitates were filtered, washed with distilled water and kept at room temperature to dry.

[VO(**L**)]: Khaki solid, yield: 72%. Dec. p.: >350 °C. Calcd. for $C_{14}H_9Cl_2NO_3V$ (%): C, 46.57; H, 2.51; N, 3.88. Found (%): C, 46.70; H, 2.58; N, 3.86. MW: 361.07 g/mol. Magnetic moment (μ_{eff}): 1.46 BM. Molar conductivity: 31.1 $\Omega^{-1}cm^2mol^{-1}$. FT-IR spectroscopy (cm^{-1}): 3071 m,br ν(CH)$_{ar.}$, 2927 m ν(CH)$_{al.}$, 1596 m ν(C=N), 1519 m ν(C=C), 1494 m, 1421 m, 1374 m, 1252 m, 1225 s ν(C–O), 1184 m, 1115 m, 992 s ν(V–O), 877 m, 842 m, 819 m, 783 s δ(CH)$_{ar.}$, 755 m ν(C–Cl), 672 m, 558 s, 469 m, 422 m. UV-vis spectra (in EtOH, λ_{max}/nm): 207 m, 278 m,br, 332 w, 437 m,br. Fluorescence spectra (λ_{max}/nm): 472 m,br

[Fe(**HL**)$_2$Cl]: Greenish black solid, yield: 70%. Dec. p.: >280 °C. Calcd. for $C_{28}H_{20}Cl_5N_2O_4Fe$ (%): C, 49.34; H, 2.96; N, 4.11. Found (%): C, 49.30; H, 2.96; N, 3.93. MW: 681.58 g/mol. Magnetic moment (μ_{eff}): 6.09 BM. Molar conductivity: 20.3 $\Omega^{-1}cm^2mol^{-1}$. FT-IR spectroscopy (cm^{-1}): 3175 m,br ν (OH), 3066 m,br ν(CH)$_{ar.}$, 2982 m ν(CH)$_{al.}$, 2920 m, 1662 m ν(C=N), 1607 m ν(C=C), 1510 m, 1423 m, 1278 m, 1205 s ν(C–O), 1169 m, 868 m, 817 m δ(CH)$_{ar.}$, 735 m ν(C–Cl), 702 s, 544 m, 516 m, 460 m. UV-vis spectra (in EtOH, λ_{max}/nm): 210 m, 228 sh, 297 m,br, 406 m,br, 528 sh. Fluorescence spectra (λ_{max}/nm): inactive

[Co(**L**)$_2$]·2H_2O: Brown solid, yield: 67%. Dec. p.: 253 °C. Calcd. for $C_{28}H_{24}Cl_4N_2O_6Co$ (%): C, 49.08; H, 3.53; N, 4.09. Found (%): C,

48.70; H, 3.39; N, 3.80. MW: 685.26 g/mol. Magnetic moment (μ_{eff}): 3.54 BM. Molar conductivity: 29.0 $\Omega^{-1}cm^2mol^{-1}$. FT-IR spectroscopy (cm^{-1}): 3227 m,br ν(OH), 3076 m,br $\nu(CH)_{ar.}$, 2982 m $\nu(CH)_{al.}$, 1616 m ν(C=N), 1591 m ν(C=C), 1492 m, 1436 s, 1249 m, 1232 m, 1201 m ν(C–O), 1177 m, 845 m, 815 m $\delta(CH)_{ar.}$, 747 s ν(C–Cl), 657 m, 549 m, 449 m. UV-vis spectra (in EtOH, λ_{max}/nm): 206 m, 249 m, 298 m,br, 353 m,br, 377 w,br, 443 m,br. Fluorescence spectra: 539 w,br

[Ni(**L**)$(H_2O)_3$]·H_2O: Mustard colored solid, yield: 64%. Dec. p.: 243 °C. Calcd. for $C_{14}H_{17}Cl_2NO_6Ni$ (%): C, 39.58; H, 4.03; 3.30. Found (%): C, 38.80; H, 3.69; N, 3.53. MW: 424.9 g/mol. Magnetic moment (μ_{eff}): 2.47 BM. Molar conductivity: 11.3 $\Omega^{-1}cm^2mol^{-1}$. FT-IR spectroscopy (cm^{-1}): 3323 m,br ν(OH), 3069 w $\nu(CH)_{ar.}$, 2964 m $\nu(CH)_{al.}$, 1621 m ν(C=N), 1576 m ν(C=C), 1519 m, 1419 m, 1394 m, 1367 m, 1270 m, 1215 m ν(C–O), 1162 m, 1128 m, 941 m, 864 m, 826 m $\delta(CH)_{ar.}$, 753 s ν(C–Cl), 645 m, 542 m, 517 m, 500 m, 462 m, 417 m. UV-vis spectra (in EtOH, λ_{max}/nm): 208 m, 215 m, 241 m,br, 258 sh, 301 w,br, 356 w, 440 m,br, 496 sh. Fluorescence spectra (λ_{max}/nm): 538 w,br.

[Cu(**L**)(H_2O)]: Khaki green solid. Yield: 78%. Dec. p.: 358 °C. Calcd. for $C_{14}H_{11}Cl_2NO_3Cu$ (%): C, 44.76; H, 2.95; N, 3.73. Found (%): C, 45.10; H, 2.78; N, 3.74. MW: 375.7 g/mol. Magnetic moment (μ_{eff}): 1.17 BM. Molar conductivity: 3.3 $\Omega^{-1}cm^2mol^{-1}$. FT-IR spectroscopy (cm^{-1}): 3354 m,br ν(OH), 3067 w $\nu(CH)_{ar.}$, 2926 m $\nu(CH)_{al.}$, 1613 m ν(C=N), 1599 m ν(C=C), 1495 m, 1443 s, 1373 m, 1269 m, 1232 m, 1202 m ν(C–O), 1173 m, 944 m, 854 m, 819 m $\delta(CH)_{ar.}$, 773 s ν(C–Cl), 758 m, 664 m, 577 m, 556 s, 505 m, 451 m, 407 m. UV-vis spectra (in EtOH, λ_{max}/nm): 202 s, 212 m, 238 m, 270 sh, 312 w,br, 435 m,br, 454 m,br, 558 w,br. Fluorescence spectra (λ_{max}/nm): 474 m,br

[Zn(**L**)(H_2O)]·$3H_2O$: Dark yellow solid. Yield: 71%. Dec. p.: 246 °C. Calcd. for $C_{14}H_{17}Cl_2NO_6Zn$ (%): C, 39.00; H, 3.97; N, 3.25. Found (%): C, 39.40; H, 3.90; N, 3.11. MW: 431.60 g/mol. Molar conductivity: 21.0 $\Omega^{-1}cm^2mol^{-1}$. FT-IR spectroscopy (cm^{-1}): 3300 m,br ν(OH), 3075 w $\nu(CH)_{ar.}$, 2923 m $\nu(CH)_{al.}$, 1648 w ν(C=N), 1602 m ν(C=C), 1493 m, 1437 s, 1370 m, 1304 m, 1258 m, 1202 m ν(C–O), 1170 m, 949 m, 816 m $\delta(CH)_{ar.}$, 768 s ν(C–Cl), 536 m, 498 m, 415 m. ^{1}H-NMR spectroscopy (ppm, 500 MHz, in DMSO-d_6): 8.94 s (1H, N=CH), 7.48 d (1H, J=3.2, H4'), 7.43 s (1H, H6'), 7.34 s (1H, H3), 7.17 s,br (1H, H5), 6.88 d (1H, J=8.3, H6), 2.22 s (3H, CH_3). ^{13}C-NMR (ppm, 125 MHz, in DMSO-d_6): 163.9 (N=CH), 158.8 (C–OH(2)), 142.6 (C–OH(1')), 140.0 (C–N=CH), 134.9 (C–CH_3), 133.7 (C4'), 133.1 (C5), 131.6 (C6'), 130.2 (C5'), 127.6 (C3'), 121.7 (C3), 119.6 (C1'), 115.5 (C6), 21.0 (CH_3). UV-vis spectra (in EtOH, λ_{max}/nm): 205 m, 211 m, 236

m,br, 299 w,br, 360 w, 432 m,br, 497 sh. Fluorescence spectra (λ_{max}/nm): 497 w,br

K[Pd(**L**)Cl]: Light brown solid. Yield: 74%. Dec. p.: >325 °C. Calcd. for $C_{14}H_9Cl_3KNO_2Pd$ (%): C, 35.39; H, 1.91; N, 2.95. Found (%): C, 35.50; H, 2. 30; N, 2.99. MW: 475.10 g/mol. Molar conductivity: 57.3 $\Omega^{-1}cm^2mol^{-1}$. FT-IR spectroscopy (cm^{-1}): 3072 w $\nu(CH)_{ar.}$, 2926 m $\nu(CH)_{al.}$, 1610 m ν(C=N), 1597 m ν(C=C), 1493 s, 1439 m, 1310 m, 1256 m, 1230 m ν(C–O), 1178 m, 920 m, 835 m, 813 m $\delta(CH)_{ar.}$, 776 s ν(C–Cl), 654 m, 577 m, 550 m, 499 m, 441 m, 405 m. ^{1}H-NMR spectroscopy (ppm, 500 MHz, in DMSO-d_6): 8.66 s (1H, N=CH), 7.72 d (1H, J=2.4, H4'), 7.68 s (1H, H6'), 7.51 d (1H, J=2.4, H3), 6.82 d (1H, J=8.3, H5), 6.60 d (1H, J=8.3, H6), 2.24 s (3H, -CH_3). ^{13}C-NMR (ppm, 125 MHz, in DMSO-d_6): 166.3 (N=CH), 156.4 (C–OH(2)), 145.8 (C–OH(1')), 139.2 (C–N=CH), 132.2 (C–CH_3), 131.8 (C4'), 130.8 (C5), 125.9 (C6'), 123.42 (C5'), 123.37 (C3'), 118.1 (C3), 116.7 (C1'), 116.6 (C6), 20.6 (CH_3). UV-vis spectra (in EtOH, λ_{max}/nm): 205 m, 212 m, 239 m, 302 w, 317 m, 332 m, 433 m,br, 456 m,br. Fluorescence spectra (λ_{max}/nm): 520 w,br

[Hg(**L**)]: black solid. Yield: 70%. Dec. p.: 185 °C. Calcd. for $C_{14}H_9Cl_2NO_2Hg$ (%): C, 33.99; H, 1.83; N, 2.83. Found (%): C, 34.45; H, 1.97; N, 2.71. MW: 494.72 g/mol. Molar conductivity: 25.0 $\Omega^{-1}cm^2mol^{-1}$. FT-IR spectroscopy (cm^{-1}): 3074 m $\nu(CH)_{ar.}$, 2977 m $\nu(CH)_{al.}$, 1660 m ν(C=N), 1607 m ν(C=C), 1567 m, 1420 m, 1372 m, 1273 m, 1206 m ν(C–O), 1169 m, 934 m, 890 m, 812 m $\delta(CH)_{ar.}$, 732 m ν(C–Cl), 702 s, 565 m, 516 m, 477 m, 432 m, 417 m. ^{1}H-NMR spectroscopy (ppm, 500 MHz, in DMSO-d_6): 10.14 s (1H, N=CH), 7.90 d,br (1H, J=1.4, H4'), 7.73 d,br (1H, H6'), 7.35 s (1H, H3), 7.07 d,br (1H, J=7.7, H5), 6.91 d,br (1H, J=6.4, H6), 2.25 s (3H, CH_3). ^{13}C-NMR (ppm, 125 MHz, in DMSO-d_6): 164.1 (N=CH), 155.3 (C–OH(2)), 145.6 (C–OH(1')), 139.8 (C–N=CH), 135.5 (C–CH_3), 129.5 (C4'), 128.0 (C5), 127.4 (C6'), 125.8 (C5'), 124.7 (C3'), 124.1 (C3), 123.7 (C1'), 115.1 (C6), 21.3 (CH_3). UV-vis spectra (in EtOH, λ_{max}/nm): 210 m, 257 m, 284 w, 343 m, 455 w,br. Fluorescence spectra (λ_{max}/nm): 533 w,br

Determination of Antibacterial and Antifungal Activity

Antibacterial activity of samples was studied *in vitro* with microbroth dilution technique against *Staphylococcus aureus* ATCC 29213 (meticillin susceptible *Staphylococcus aureus*, MSSA*), Enterococcus facealis* ATCC 29212, *Escherichia coli* ATCC 25922, *Klebsiella pneumonia* ATCC 4352, *Pseudomonas aeruginosa* ATCC 27853, *Staphylococcus epidermidis* ATCC 12228. Antifungal activity was assayed *in vitro* against *Candida albicans* ATCC 10231, *Candida parapsilosis* ATCC

22019 and *Candida tropicalis* ATCC 750. The evaluation of antibacterial and antifungal activity was done using micro broth dilution technique according to the Clinical Laboratory Standards Institute (CLSI) guidance [34, 35]. As a test medium, Mueller-Hinton broth for bacteria and Roswell Park Memorial Institute (RPMI-1640) medium for yeast were used. In the medium serial two-fold dilutions were prepared beginning from 5000 to 4.9 μg/cm^3. The inoculum was prepared using 18 – 20 h broth culture of each bacteria type and 24 h culture of yeast strains adjusted to a turbidity equivalent to 0.5 McFarland standard, diluted in broth media to give a final concentration of 5×10^5 cfu/cm^3 for bacteria and 5×10^3 cfu/cm^3 for yeast in the test tray. To prevent evaporation, trays were covered and placed into plastic bags. The trays containing Mueller-Hinton broth were incubated at 37 °C for 18 – 20 h while the trays containing RPMI-1640 medium were incubated at 25 °C for 46 – 50 h. The antimicrobial effects of the solvents were measured against test strains as a control, and according to the values of the controls, minimum inhibitory concentrations (MICs) of the compounds were determined. The MIC was defined as the lowest concentration of compound giving total inhibition of visible growth. The MIC values of the compounds are given in **Table 1**.

The samples were evaluated for their antibacterial and antifungal potency against members of Gram-negative bacteria, Gram-positive bacteria, and Candida spp. As reference compounds, Ciprofloxacin for antibacterial assays, and Amphotericin B for antifungal assays were preferred.

Antioxidant Efficiency

The antioxidant efficiencies of the ligands and metal complexes were evaluated using the Cupric Reducing Antioxidant Capacity (CUPRAC) method. The CUPRAC method involves the reduction of the Cu(II)-Neocuproine complex to the yellow-orange Cu(I)-Neocuproine complex in the presence of antioxidants, with the change in absorbance recorded at a wavelength of 450 nm [36, 37] and the micromolar trolox equivalent antioxidant capacity (TEAC) was determined in μM.

DPPH Radical Scavenging Activity

One mM of purple colored DPPH (1,1-diphenyl-2-picrylhydrazyl) radical, DPPH•) solution was diluted at a ratio of 1:10 (v:v) with ethanol. To a tube, x mL of sample, 1 mL of DPPH• solution and $(4 - x)$ mL of ethanol were added and the mixture was kept for 30 min at room temperature. The sample solutions were spectrophotometrically measured against ethanol at 525 nm. The concentrations corresponding to the absorbances found were plotted, and the percent inhibition values were calculated

according to the literature [38]. The inhibition values were calculated using the equation below:

$$\text{Inhibition (\%)} = 100\ (A_o - A) / A_o$$

Results and discussion

General Properties of the Compounds

In this study, eight related transition metal complexes were obtained by allowing the **H_2L** ligand to react with VO(II), Fe(III), Co(II), Ni(II), Cu(II), Zn(II), Pd(II) and Hg(II) ions at a molar ratio of 1:1. The ligand is tridentate and has dibasic chelating characteristics.

The M:L ratio is 1:2 in the Fe(III) and Co(II) complexes and 1:1 in the other complexes. According to the molar conductivity measurements, the Pd(II) complex has 57.3 $\Omega^{-1}cm^2mol^{-1}$ molar conductivity is 1:1 ionic, whereas the other complexes with molar conductivity values ranging from 3.3 to 31.1 $\Omega^{-1}cm^2mol^{-1}$ are non-ionic [39]. The ligands gave immediately khaki green colored precipitates with $CuCl_2$, forming a strong chelate in EtOH. They showed also similar behavior towards K_2PdCl_4, $VOSO_4$ and $HgCl_2$. Co(II), Ni(II) and Zn(II) ions reacted with the ligands differently from these two metals under reaction conditions. It was observed that these metal salts did not form complexes in ethanol, where they were dissolved with the ligand, due to the low pH value of the medium (pH = ~4.5). Therefore, the pH value of the medium was brought to the range of 5.5-6 by using 5% methanolic NaOH solution and it was observed that the mentioned complexes were formed in this medium.

Room temperature magnetic moment value of the vanadyl(IV) complex is 1.46 BM for a 1:1 monomeric structure. Although this value is lower than the theoretical value of 1.71 BM for the VO(II) ion with d^1 electronic configuration, it remains within acceptable limits due to the influence of various factors. A magnetic moment value of 6.09 BM was obtained for the Fe(III) complex, indicating a typical monomeric high-spin Fe(III) complex. Theoretical magnetic moment value of a system with five unpaired electrons is 5.9 BM, and the value of Fe(III) complex we found is very close to this. The magnetic moment value of the copper(II) complex was found to be 1.17 BM, which is much lower than the expected value and must have resulted from between two Cu(II) ion interaction. The complex may have a dimeric structure and as a result, there is an antiferromagnetic interaction between Cu(II)–Cu(II) ions, causing the magnetic moment value to be lower than expected [40]. Considering that the ligand is tridentate, it is possible to suggest that the Cu(II) complex has a five-coordination structure bridged over water molecules [41].

Magnetic moment value was found to be 3.54 BM for $[Co(\mathbf{L})_2]\cdot 2H_2O$. This can be considered as evidence that the five coordinated d^7 complex is in a high spin structure (three

unpaired electrons). The geometry of the central ion may be octahedral. The nickel(II) complex has 2.47 BM magnetic moment value lower than the expected one for an octahedral or tetrahedral d^8 ion (expected value for 2 unpaired electrons is 2.83 BM). This value can be considered to result from a distorted geometry between tetrahedral and square planar systems, called quasi-tetrahedral [42–44].

Infrared Spectroscopy

IR spectroscopy data of the obtained compounds are presented in Experimental section. By comparing the IR spectra of **H_2L** and its complexes, the IR spectral changes that occurred as a result of complexation were determined. The medium bands appearing at 1636 and 1615 cm^{-1} in the ligand must belong to the azomethine HC=N and C=C bonds, respectively. The band belonging to the C=N bond undergoes a significant change in complexes, its intensity weakens and it shifts to lower or higher wave numbers. The medium band seen at 3192 cm^{-1} in the ligand belongs to the OH stretching vibration and disappears as a result of the coordination of phenolic oxygen atoms in the complexes. The medium bands seen between 3200 – 3350 cm^{-1} in complexes containing water, that is, Co(II), Ni(II), Cu(II) and Zn(II) complexes, arise from the stretching vibrations of water molecules. The absence of any bands in the VO(II), Pd(II) and Hg(II) complexes in this region indicates that there are no water molecules, coordinated or not and hydrogen bonds in these complexes.

The medium band appears at 1200 cm^{-1} can be assigned to the phenolic C–O group stretching vibration. This band shows significant changes in the complexes, which can be said to be due to the coordination of phenolic oxygen and the removing of the proton. In the vanadyl(IV) complex, the characteristic stretching vibration band of the V=O bond is seen as a strong peak at 992 cm^{-1}. The comparative IR spectra of **H_2L** and its complexes are given in **Figure 2**.

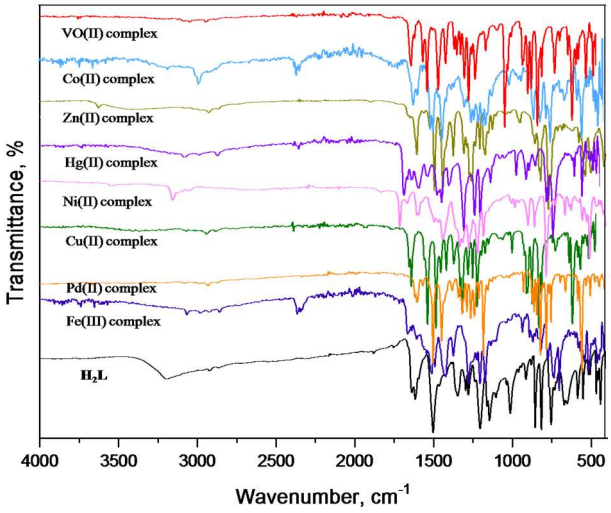

Figure 2. Comparative FTIR spectra of **H_2L** and its complexes

NMR Spectroscopy

NMR spectroscopy data of the obtained compounds are given in Experimental section. In the ^{1}H-NMR spectra of the ligand, one of the phenolic OH protons (OH1', salicyl OH) could

not be detected, possibly due to dissociation, while the signal of the other (OH2, phenolic OH) appeared at 9.98 ppm. The imino hydrogen (–CH=N–) of **H_2L** was observed at 9.08 ppm. As a result of the formation of the complexes, OH protons were not detected in the zinc(II) complex, while the proton of –CH=N– group shifted to a low ppm value: it was detected at 8.94 and 8.66 ppm as singlet in the Zn(II) and Pd(II) complexes of **H_2L**, respectively. **Figure 3** shows the ^{1}H-NMR spectra of the ligand and the Zn(II) complex comparatively.

Similarly, in the ^{13}C-NMR spectra, it is seen that the carbon atoms most affected by the complex formation are the carbon atoms attached to the OH groups and the imine carbon atom (–CH=N–). The imine carbon atoms are detected at 160.4 ppm in **H_2L** and at 166.3, 164.1 and 163.9 ppm in its palladium(II), mercury(II) and zinc(II) complexes, respectively. The C1'–OH and C2–OH carbon atoms of **H_2L** appeared at 149.1 and 158.9 ppm, respectively, and shifted to the lower ppm values in the complexes.

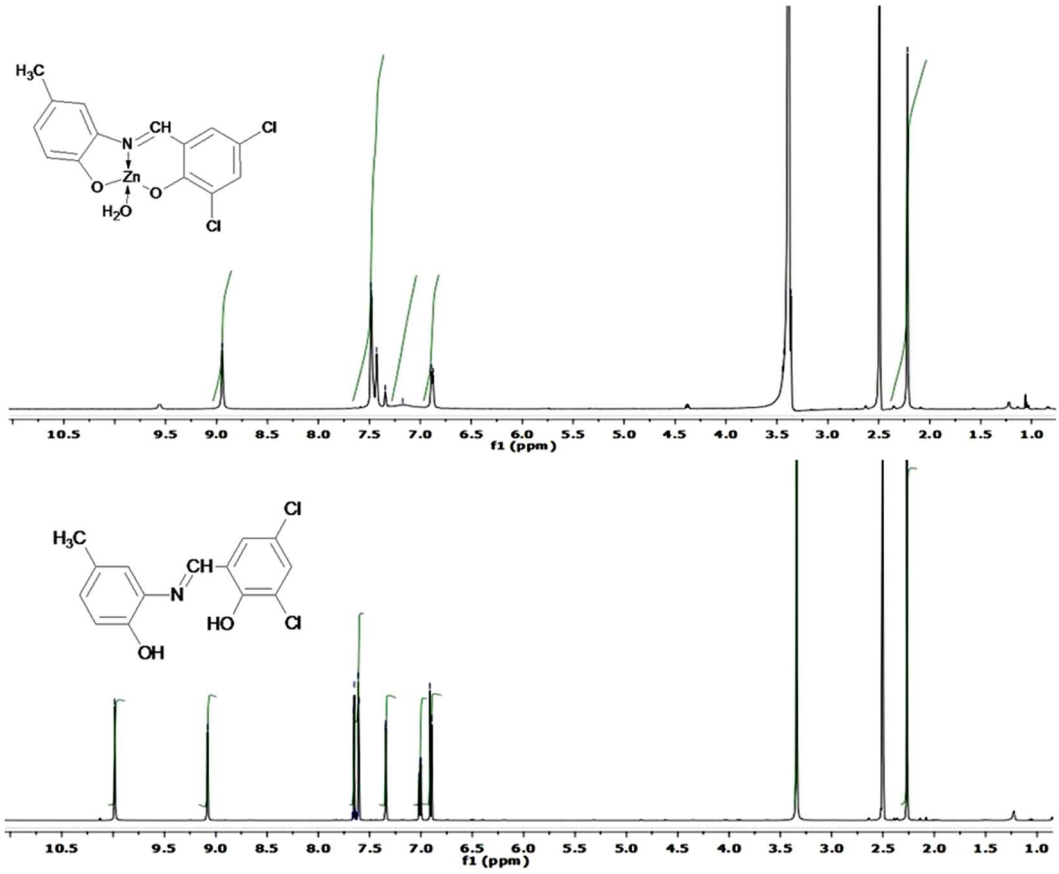

Figure 3. ^{1}H-NMR spectra of **H_2L** and its Zn(II) complex in DMSO-d_6.

UV-Visible and Fluorescence Spectroscopy

UV-visible and fluorescence data of the compounds obtained in ethanol are presented in Experimental Section.

The electronic spectra of the compounds exhibit intense bands at the 200 – 290 nm region: The bands between 200 and 250 nm are due to $\pi \rightarrow \pi^*$ transitions in the aromatic rings. The bands at the 250 – 300 nm range correspond to $\pi \rightarrow \pi^*$ transitions of azomethine group, whereas the bands at the 300 – 350 nm range correspond to the $n \rightarrow \pi^*$ transitions [45].

The bands at 469 (m,br) and 497 nm (sh) in the ligand are related to intraligand charge transfer transitions. The band at 456 nm in the spectra of Pd(II) complex indicate square planar stereochemistry and can be assigned to $^1A_{1g} \rightarrow {}^1A_{2g}$ transition. The band at 454 nm for the Cu(II) complex can be attributed to *d – d* transitions and it may be considered as an indication that this complex has distorted square pyramidal geometry [46–48]. The absorption seen at 443 nm in the Co(II) complex may belong to $^4T_{1g}(F) \rightarrow {}^4T_{1g}(P)$ transition for d^7 ion in octahedral field [49]. The other octahedral field transitions could not be detected for the Co(II) complex. Since there are no allowed *d – d* transitions in the Zn(II) and Hg(II) complexes, the bands at the 350 – 500 nm range arise from the intraligand and metal-to-ligand charge transfer transitions. The absorptions observed at 406 and 528 nm in the Fe(III) complex should be belong to the LMCT and *d – d* transitions, respectively [50]. It is possible to attribute the absorption band appearing at 437 nm in the VO(II) complex, which is expected to have a tetrahedral structure, to the LMCT band [51]. The comparative UV-vis spectra of **H_2L** and its complexes are given in **Figure 4**.

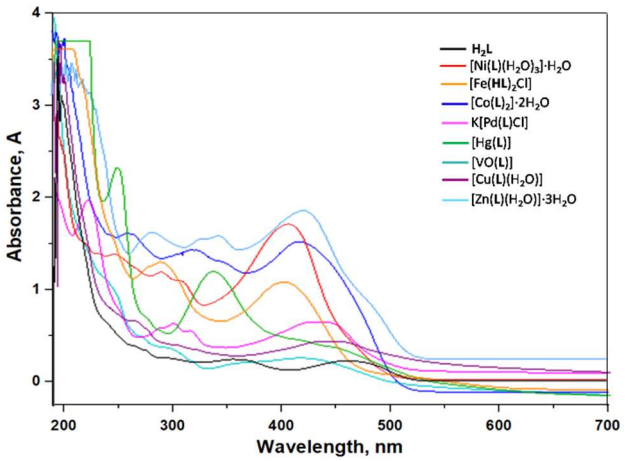

Figure 4. The comparative UV-vis spectra of **H_2L** and its complexes

Schiff base derivatives containing nitrogen-oxygen rich coordination as a receptor site pave a considerable platform for fluorescent sensing with strong noticeable color change [52]. **H_2L** shows weak fluorescence characteristic in the neutral state; it shows relatively more intense fluorescence in the acidic and basic regions. At the same time, the emission wavelength shifts to a lower wavelength (red shift) in both acidic and basic areas (more shifts in acidic region). The fluorescence spectra of **H_2L** in neutral, acidic and basic environments are given in **Figure 5**. It is

seen that Cu(II) and VO(II) complexes differ from the others in terms of both red shift (474 and 472 nm, respectively) and more intense fluorescence properties (Fig. 6). In other words, it seems that the ligand behaves differently towards Cu(II) and VO(II) ions than the others. Considering that it reacts strongly with Cu(II) and VO(II) ions, it is possible to argue that this and similar Schiff bases will be useful in detecting these metal ions.

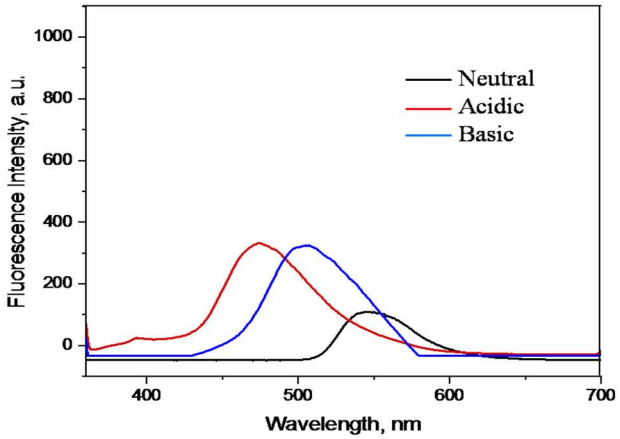

Figure 5. The fluorescence spectra of **H_2L** in neutral, acidic and basic environments

The Fe(III) complex differs from the others by not showing fluorescence characteristic. Due to this feature, it is possible to assert that **H_2L** and similar Schiff bases show good selectivity for Fe(III) ions. In addition, it is noteworthy that in all complexes except the Fe(III) complex, the fluorescence emission occurs at a lower wavelength (red shift) compared to the ligand. The fluorescence spectra of **H_2L** with its metal complexes are comparatively given in **Figure 6**.

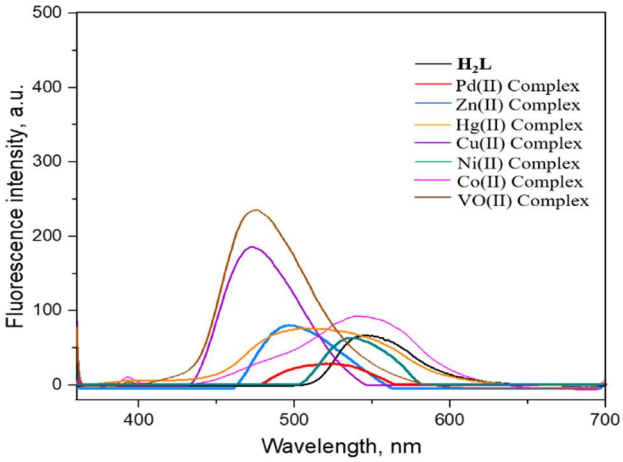

Figure 6. Comparative fluorescence spectra of **H_2L** and its metal complexes

In the light of the analytical and spectroscopic data obtained, the proposed structures in **Figure 7** can be suggested for the complexes in the study.

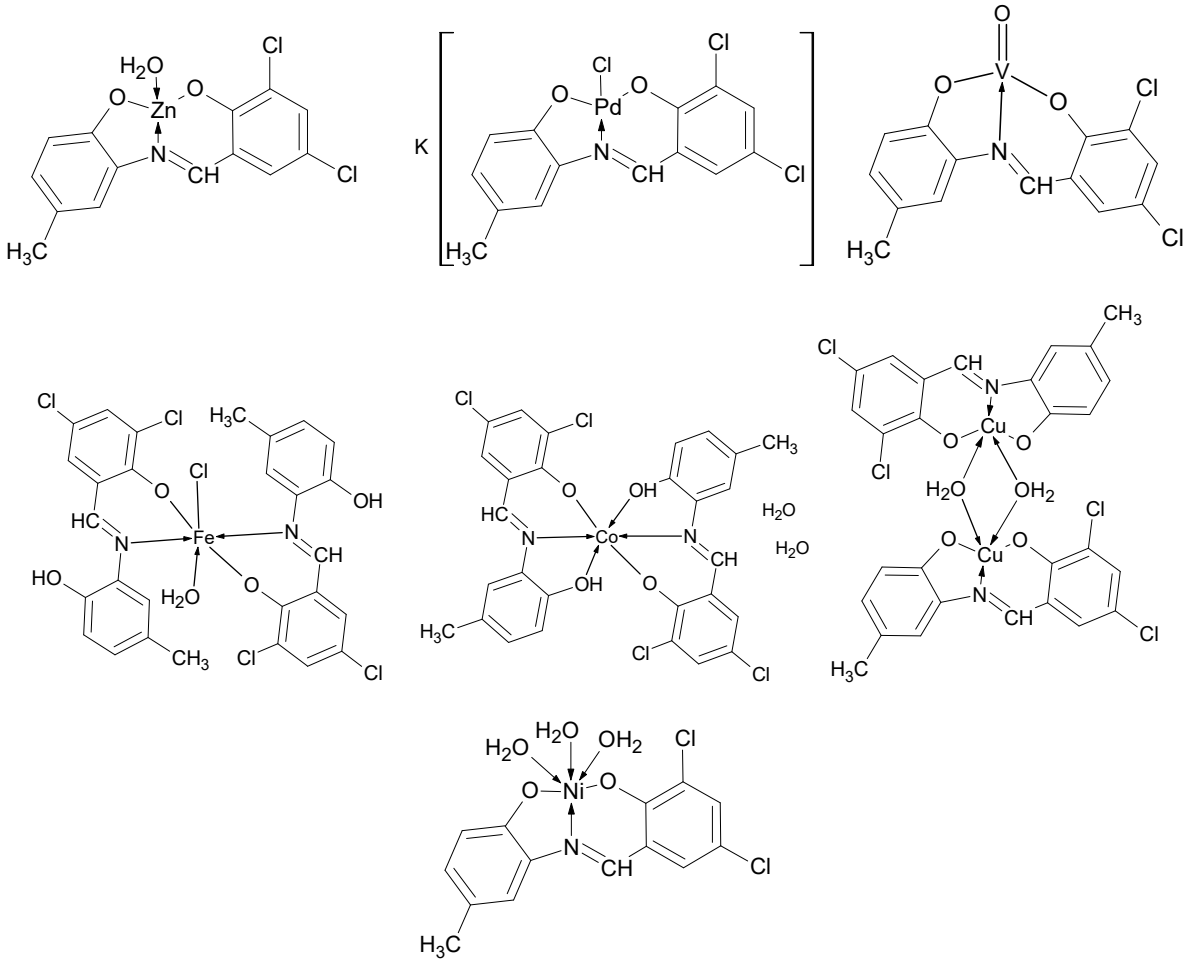

Figure 7. The proposed structures showing coordinations for the complexes

Antimicrobial Activity

In vitro antimicrobial activity test results of **H_2L** and its metal complexes in terms of MIC are presented in Table 1 in comparison with the values of the antibiotics and antifungal agents.

It is seen that the all the complexes show moderate or weak activity against the test microorganisms. It was observed that VO(II), Co(II), Cu(II) and Zn(II) complexes showed higher activity than the ligands, especially against Gram+ bacteria *S. aureus* and *S. epidermidis*. Another noteworthy result is that the Cu(II) complex has higher activity against *C. albicans* and the Pd(II) complex has higher activity than the ligand against all three fungi. Similar antifungal activity results to those of our compounds are also found in the literature [53, 54]. It would also be appropriate to mention that the Cu(II) complex is more active against *P. aeruginosa* and the Pd(II) complex is more active against *E. coli* than the ligand. The results we obtained here, again with ONO type Schiff bases, were found to be mediocrely effective, as in our previous studies [11, 48].

Table 1. *In vitro* antimicrobial activity of the compounds (MIC, µg/mL)

Compound	----------Bacteria----------						-------Fungi------		
	Sa[*,a]	*Se*[a]	*Kp*[b]	*Ec*[b]	*Pm*[b]	*Pa*[b]	*Cp*	*Ct*	*Ca*
H_2L	625	313	313	625	625	625	625	625	625
[VO(**L**)]	313	156	2500	1250	1250	625	625	625	1250
[Fe(**HL**)$_2$Cl]	313	313	1250	1250	1250	1250	1250	1250	1250
[Co(**L**)$_2$]·2H_2O	313	156	1250	625	1250	1250	1250	1250	1250
[Ni(**L**)(H_2O)$_3$]·H_2O	156	156	2500	1250	625	1250	1250	1250	625
[Cu(**L**)(H_2O)]	156	313	625	625	1250	313	625	1250	156
[Zn(**L**)(H_2O)]·3H_2O	156	156	2500	625	1250	625	1250	1250	625
K[Pd(**L**)Cl]	1250	625	1250	313	625	625	313	156	156
[Hg(**L**)]	313	313	1250	1250	1250	1250	1250	1250	625
References[c]	0.25	0.25	0.007	0.007	0.125	0.007	0.5	1.0	1.0

* *Sa Staphylococcus aureus* ATCC 6538 *Se Staphylococcus epidermidis* ATCC 12228
Ec Escherichia coli ATCC 8739 *Kp Klebsiella pneumoniae* ATCC 4352
Pa Pseudomonas aeruginosa ATCC 1539 *Pm Proteus mirabilis* ATCC 14153
Ca Candida albicans ATCC 10231 *Cp Candida parapsilosis* ATCC 22019
Ct Candida tropicalis ATCC 750
[a]: Gram+; [b]: Gram–. [c]: Ciprofloxacin and Amphotericin B were used for bacteria and fungi, respectively.

Antioxidant Activity

The antioxidant activities of the compounds were tested by 1,1-diphenyl-2-picrylhydrazyl radical (DPPH•) scavenging activity and Cupric Reducing Antioxidant Capacity (CUPRAC) assays and the results are given in **Table 2**.

As shown in **Table 2**, Co(II), Cu(II), Zn(II), VO(II) and Pd(II) complexes exhibited significantly higher Trolox equivalent antioxidant capacity (TEAC) values compared to the ligand. These results indicate a substantial increase in antioxidant efficiency with these complexes. On the other hand, antioxidant efficiency remained nearly unchanged with iron(III) and nickel(II) complexes, while a decrease was observed with the mercury(II) complex.

Table 2. The TEAC and DPPH radical scavenging values of the ligand and the complexes

Compounds	TEAC value (mg/mL)	DPPH radical scavenging (%)
H_2L	1.830	57.76
[Fe(**HL**)$_2$Cl]	2.140	8.56
[Co(**L**)$_2$]·2H_2O	4.491	49.63
[Ni(**L**)(H_2O)$_3$]·H_2O	1.557	21.22
[Cu(**L**)(H_2O)]	6.825	32.38
[Zn(**L**)(H_2O)]·3H_2O	7.713	89.95
[VO(**L**)]	6.359	39.83
[Hg(**L**)]	0.728	10.30
K[Pd(**L**)Cl]	7.421	37.17

It was observed that the sample of Zn(II) complex in DMF solution showed the highest DPPH radical scavenging activity with an 89.95% value. It was observed that Fe(III), Ni(II) and Hg(II) complexes showed low radical scavenging activity compared to the other complexes. In addition, another noteworthy result is that Ni(II) and Hg(II) complexes showed lower antioxidant activity than the ligand. Similar antioxidant effects were reported in the literature for some ONO type Schiff base ligands and their complexes [55, 56].

Conclusions

Schiff bases derived from salicylaldehyde are compounds that attract attention due to their chelation structures as ligands, their variety of uses, and many interesting properties. In this context, we synthesized a new salicyl based imine compound (**H_2L**) derived from 3,5-dichlorosalicylaldehyde and 4-methyl-2-aminophenol and characterized by some physicochemical and spectral techniques. Then, we prepared the complexes of **H_2L** with $VOSO_4$, $FeCl_3$, MCl_2, (M = Co, Ni, Cu, Zn and Hg) and K_2PdCl_4 and characterized with elemental analysis, molar conductivity, magnetic moment, FT-IR and NMR spectroscopy. The metal:ligand ratio is 1:2 in Fe(III) and Co(II) complexes whereas 1:1 in the other complexes. According to molar conductance values, the Pd(II) complex is 1:1 ionic and the other complexes are non-ionic. It was observed that fluorescence character of **H_2L**, which shows weak fluorescence, increased in its VO(II) and Cu(II) complexes, was quenched in the Fe(III) complex, and weakened in other complexes. Antibacterial and antifungal activity of the compounds was evaluated against six bacteria and three fungi and found that all the compounds showed moderate antimicrobial activity. VO(II), Co(II), Cu(II) and Zn(II) complexes showed higher activity than the ligands against Gram+ bacteria. Antioxidant activities of the compounds were investigated by applying DPPH• scavenging and CUPRAC methods, and it was found that Zn(II) and Pd(II) complexes showed higher antioxidant activity than the ligand and the other complexes.

Funding

This work was supported by Scientific Research Projects Coordination Unit of Istanbul University-Cerrahpasa (Project number: 36370) and The Scientific and Technological Research Council of Türkiye (TUBITAK) (Project number: 123Z795).

References

[1] Aboul-Fadl T, Mohammed F, Hassan E. Synthesis, antitubercular activity and pharmacokinetic studies of some schiff bases derived from 1- alkylisatin and isonicotinic acid hydrazide (INH). Archives of Pharmacal Research 2003;26(10):778-784.

[2] Miri R, Razzaghi-asl N, Mohammadi M. QM study and conformational analysis of an isatin Schiff base

as a potential cytotoxic agent. Journal of Molecular Modeling 2012;19(2):727-735.

[3] Ren S, Wang R, Komatsu K, Bonaz-Krause P, Zyrianov Y, McKenna C, Csipke C, Tokes Z, Lien E. Synthesis, Biological Evaluation, and Quantitative Structure−Activity Relationship Analysis of New Schiff Bases of Hydroxysemicarbazide as Potential Antitumor Agents. Journal of Medicinal Chemistry 2001;45(2):410-419.

[4] Pandeya S, Sriram D, Nath G, DeClercq E. Synthesis, antibacterial, antifungal and anti-HIV activities of Schiff and Mannich bases derived from isatin derivatives and N-[4-(4′-chlorophenyl)thiazol-2-yl] thiosemicarbazide. European Journal of Pharmaceutical Sciences 1999;9(1):25-31.

[5] da Silva CM, da Silva DL, Modolo LV, Alves RB, de Resende MA, Martins CVB, de Fatima A. Schiff bases: A short review of their antimicrobial activities. Journal of Advanced Research, 2011;2(1):1-8.

[6] Kajal A, Bala S, Kamboj S, Sharma N, Saini V. Schiff Bases: A Versatile Pharmacophore. Journal of Catalysts 2013;2013:1-14.

[7] Shi L, Ge H, Tan S, Li H, Song Y, Zhu H, Tan R. Synthesis and antimicrobial activities of Schiff bases derived from 5-chloro-salicylaldehyde. European Journal of Medicinal Chemistry 2007;42(4):558-564.

[8] Sahu R, Thakur D, P K. Schiff Base: An Overview of its Medicinal Chemistry Potential for New Drug Molecules. International Journal of Pharmaceutical Sciences and Nanotechnology 1970;5(3):1757-1764.

[9] Cozzi P. Metal–Salen Schiff base complexes in catalysis: practical aspects. Chem. Soc. Rev. 2004;33(7):410-421.

[10] Tarafder M, Jin K, Crouse K, Ali A, Yamin B, Fun H. Coordination chemistry and bioactivity of Ni2+, Cu2+, Cd2+ and Zn2+ complexes containing bidentate Schiff bases derived from S-benzyldithiocarbazate and the X-ray crystal structure of bis[S-benzyl-β-N-(5-methyl-2-furylmethylene)dithiocarbazato]cadmium(II). Polyhedron 2002;21(25-26):2547-2554.

[11] Alterhoni E, Tavman A, Gürbüz D, Hacioglu M, Çinarli A, Şahin O, Tan A. Synthesis, Characterization and Antimicrobial Activity of Schiff Bases Including Three Hydroxy Groups and Their CoCl2, PdCl2, CuCl2 and ZnCl2 Complexes. Chemistry Select 2020;5(31):9730-9735.

[12] Alterhoni E, Tavman A, Hacioglu M, Şahin O, Seher Birteksöz Tan A. Synthesis, structural characterization and antimicrobial activity of Schiff bases and benzimidazole derivatives and their complexes with CoCl2, PdCl2, CuCl2 and ZnCl2. Journal of Molecular Structure 2021;1229:129498.

[13] Fujita E, Brunschwig B, Ogata T, Yanagida S. Toward photochemical carbon dioxide activation by transition metal complexes. Coordination Chemistry Reviews 1994;132:195-200.

[14] Opstal T, Verpoort F. Synthesis of Highly Active Ruthenium Indenylidene Complexes for Atom-Transfer Radical Polymerization and Ring-Opening-Metathesis Polymerization. Angewandte Chemie International Edition 2003;42(25):2876-2879.

[15] Clercq B, Lefebvre F, Verpoort F. Immobilization of multifunctional Schiff base containing ruthenium complexes on MCM-41. Applied Catalysis A: General 2003;247(2):345-364.

[16] Tantaru G, Dorneanu V, Stan M. Schiff bis bases: analytical reagents. II. Spectrophotometric determination of manganese from pharmaceutical forms. Journal of Pharmaceutical and Biomedical Analysis 2002;27(5):827-832.

[17] McAuliffe C, Parish R, Abu-El-Wafa S, Issa R. High-valent manganese complexes of tetradentate schiff base ligands. ESR-active and ESR-silent dimeric species. Inorganica Chimica Acta 1986;115(1):91-94.

[18] Boghaei D, Mohebi S. Non-symmetrical tetradentate vanadyl Schiff base complexes derived from 1,2-phenylene diamine and 1,3-naphthalene diamine as catalysts for the oxidation of cyclohexene. Tetrahedron 2002;58(26):5357-5366.

[19] Papic S, Koprivanac N, Grabaric Z, Parac-Osterman D. Metal complex dyes of nickel with schiff bases. Dyes and Pigments, 1994;25:229-240.

[20] Nejati K, Rezvani Z, Massoumi B. Syntheses and investigation of thermal properties of copper complexes with azo-containing Schiff-base dyes. Dyes and Pigments 2007;75(3):653-657.

[21] Kumar S, Dhar DN, Saxena PN. Applications of metal complexes of Schiff bases-A review. Journal of Scientific and Industrial Research, 2009;68:181-187.

[22] Chantarasiri N, Ruangpornvisuti V, Muangsin N, Detsen H, Mananunsap T, Batiya C, Chaichit N. Structure and physico-chemical properties of hexadentate Schiff base zinc complexes derived from salicylaldehydes and triethylenetetramine. Journal of Molecular Structure 2004;701(1-3):93-103.

[23] Abdallah S, Mohamed G, Zayed M, El-Ela M. Spectroscopic study of molecular structures of novel Schiff base derived from o-phthaldehyde and 2-aminophenol and its coordination compounds together with their biological activity. Spectrochimica Acta Part A: Molecular and Biomolecular Spectroscopy 2009;73(5):833-840.

[24] Nartop D, Özdemir Ö, Gürkan P. Synthesis, characterization and investigation of tautomeric, potentiometric and antimicrobial properties of a novel unsymmetric Schiff base and its Fe (III) and Ni (II) complexes. Moroccan Journal of Chemistry, 2017;5:560-572.

[25] Cinarli A, Gürbüz D, Tavman A, Seher Birteksöz A. Synthesis, spectral characterizations and antimicrobial activity of some Schiff bases of 4-chloro-2-aminophenol. Bulletin of the Chemical Society of Ethiopia 2011;25(3):407-417.

[26] Cinarli A, Gürbüz D, Tavman A, Birteksöz A. Spectral Characterization and Antimicrobial Activity of Some Schiff Bases Derived from 4-Chloro-2-aminophenol and Various Salicylaldehyde Derivatives. Chinese Journal of Chemistry 2012;30(2):449-459.

[27] Gürbüz D, Cinarli A, Tavman A, Birteksöz A. Spectral Characterization and Antimicrobial Activity of Some Schiff Bases Derived from 4-Methyl-2-aminophenol. Chinese Journal of Chemistry 2012;30(4):970-978.

[28] Gürbüz D, Çinarli A, Tavman A, Tan ASB. Synthesis, characterization and antimicrobial activity of some transition metal complexes of N-(5-chloro-2-hydroxyphenyl)-3-methoxy-salicylaldimine. Bulletin of the Chemical Society of Ethiopia 2015;29(1):63.

[29] Kusmariya B, Mishra A. Co(II), Ni(II), Cu(II) and Zn(II) complexes of tridentate ONO donor Schiff base ligand: Synthesis, characterization, thermal, non-isothermal kinetics and DFT calculations. Journal of Molecular Structure 2017;1130:727-738.

[30] Zhang Z, Zeng H, Liu Y, Kuang D, Zhang F, Tan Y, Jiang W. Synthesis, crystal structure and anticancer activity of the dibutyltin(IV)oxide complexes containing substituted salicylaldehyde-o-aminophenol Schiff base with appended donor functionality. Inorganic and Nano-Metal Chemistry 2018;48(10):486-494.

[31] Afrin A, Jayaraj A, Gayathri M, P. C. An overview of Schiff base-based fluorescent turn-on probes: a potential candidate for tracking live cell imaging of biologically active metal ions. Sensors & Diagnostics 2023;2(5):988-1076.

[32] Lohar S, Pal S, Mukherjee M, Maji A, Demitri N, Chattopadhyay P. A turn-on green channel Zn2+ sensor and the resulting zinc(ii) complex as a red channel

HPO42− ion sensor: a new approach. RSC Advances 2017;7(41):25528-25534.

[33] Jung J, Yun D, Lee H, Kim K, Kim C. Selective chemosensor capable of sensing both CN− and Zn2+: Its application to zebrafish. Sensors and Actuators B: Chemical 2019;297:126814.

[34] Clinical and Laboratory Standards Institute (CLSI). Reference Method for Broth Dilution Antifungal Susceptibility Testing of Yeasts; Approved Standard-Third Edition. M27-A3, Wayne, PA, USA, (2012).

[35] Clinical and Laboratory Standards Institute (CLSI). Performance Standards for Antimicrobial. Document M100-Ed.31., Wayne, PA, USA (2021).

[36] Apak R, Güçlü K, Özyürek M, Karademir S. Novel Total Antioxidant Capacity Index for Dietary Polyphenols and Vitamins C and E, Using Their Cupric Ion Reducing Capability in the Presence of Neocuproine: CUPRAC Method. Journal of Agricultural and Food Chemistry 2004;52(26):7970-7981.

[37] Apak R, Güçlü K, Özyürek M, Esin Karademir S, Erçağ E. The cupric ion reducing antioxidant capacity and polyphenolic content of some herbal teas. International Journal of Food Sciences and Nutrition 2006;57(5-6):292-304.

[38] Sánchez-Moreno C, Larrauri J, Saura-Calixto F. A procedure to measure the antiradical efficiency of polyphenols. Journal of the Science of Food and Agriculture 1998;76(2):270-276.

[39] Geary W. The use of conductivity measurements in organic solvents for the characterisation of coordination compounds. Coordination Chemistry Reviews 1971;7(1):81-122.

[40] Amer S, El-Wakiel N, El-Ghamry H. Synthesis, spectral, antitumor and antimicrobial studies on Cu(II) complexes of purine and triazole Schiff base derivatives. Journal of Molecular Structure 2013;1049:326-335.

[41] Ahmad Mantoo I, Bashir M, Yousuf I. A novel diaqua−bridged water soluble copper(II) complex acts as an efficient cytotoxic agent against lung cancer cells. Inorganic Chemistry Communications 2023;157:111384

[42] Lomjanský D, Rajnák C, Titiš J, Moncoľ J, Smolko L, Boča R. Impact of tetrahedral and square planar geometry of Ni(II) complexes with (pseudo)halide ligands to magnetic properties. Inorganica Chimica Acta 2018;483:352-358.

[43] Starikov A, Minyaev R, Minkin V. Theoretical modeling of the square-planar to tetrahedral isomerization of bis-chelate nickel(II) complexes. Chemical Physics Letters 2008;459(1-6):27-32.

[44] Bridgeman A. On the origin of paramagnetism in planar nickel(ii) complexes. Dalton Transactions 2008;(15):1989.

[45] Kaya Y, Mutlu H, Irez G. Uv-vis spectra and fluorescence properties of two iminooxime ligands and their metal complexes: optical band gaps. Gazi University Journal of Science, 2010;23:13-18.

[46] Mautner F, Fischer R, Torvisco A, Henary M, Louka F, Massoud S, Salem N. Five-Coordinated Geometries from Molecular Structures to Solutions in Copper(II) Complexes Generated from Polydentate-N-Donor Ligands and Pseudohalides. Molecules 2020;25(15):3376.

[47] Khan S, Al Masum A, Islam M, Drew M, Bauzá A, Frontera A, Chattopadhyay S. Observation of π-hole interactions in the solid state structures of three new copper(II) complexes with a tetradentate N4 donor Schiff base: Exploration of their cytotoxicity against MDA-MB 468 cells. Polyhedron 2017;123:334-343.

[48] Pardaeva D, Tavman A, Gürbüz D, Hacioglu M, Yilmaz FN, Şahin O, Tan ASB, Çinarli, A. Spectral characterization and antibacterial, antifungal, antiviral activity of salicyl based new Schiff bases and their Co(II),

Ni(II), Cu(II), Zn(II), and Pd(II) complexes. Revue Roumaine de Chimie, 2024;69:83-96.

[49] Jain P, Sharma S, Kumar N, Misra N. Ni(II) and Cu(II) complexes of bidentate thiosemicarbazone ligand: Synthesis, structural, theoretical, biological studies and molecular modeling. Applied Organometallic Chemistry 2020;34(9):e5371.

[50] Abu-Dief A, Abdel-Rahman L, Abdelhamid A, Marzouk A, Shehata M, Bakheet M, Almaghrabi O, Nafady A. Synthesis and characterization of new Cr(III), Fe(III) and Cu(II) complexes incorporating multi-substituted aryl imidazole ligand: Structural, DFT, DNA binding, and biological implications. Spectrochimica Acta Part A: Molecular and Biomolecular Spectroscopy 2020;228:117700.

[51] Abdel-Rahman L, Abu-Dief A, Moustafa H, Abdel-Mawgoud A. Design and nonlinear optical properties (NLO) using DFT approach of new Cr(III), VO(II), and Ni(II) chelates incorporating tri-dentate imine ligand for DNA interaction, antimicrobial, anticancer activities and molecular docking studies. Arabian Journal of Chemistry 2020;13(1):649-670.

[52] Udhayakumari D, Inbaraj V. A Review on Schiff Base Fluorescent Chemosensors for Cell Imaging Applications. Journal of Fluorescence 2020;30(5):1203-1223.

[53] Devi J, Yadav M, Kumar D, Naik L, Jindal D. Some divalent metal(II) complexes of salicylaldehyde-derived Schiff bases: Synthesis, spectroscopic characterization, antimicrobial and in vitro anticancer studies. Applied Organometallic Chemistry 2018;33(2):e4693.

[54] Abdel Aziz A, Salem A, Sayed M, Aboaly M. Synthesis, structural characterization, thermal studies, catalytic efficiency and antimicrobial activity of some M(II) complexes with ONO tridentate Schiff base N-salicylidene-o-aminophenol (saphH2). Journal of Molecular Structure 2012;1010:130-138.

[55] Oloyede-Akinsulere A, Olalekan Babajide J, Olonkwoh Salihu S. Synthesis, Antibacterial and Antioxidant Activities of Some Tridentate Substituted Salicylaldimines. Asian Journal of Applied Chemistry Research 2018;1(4):1-10.

[56] Aslam M, Anis I, Mehmood R, Iqbal L, Iqbal S, Khan I, Chishti M, Perveen S. Synthesis and biological activities of 2-aminophenol-based Schiff bases and their structure–activity relationship. Medicinal Chemistry Research 2015;25(1):109-115.